Journal of Energy and Natural Resources
2024, Vol. 13, No. 2, pp. 50-58
https://doi.org/10.11648/j.jenr.20241302.11

Research Article

Dissecting of Atomic Morphology of Superfine Pulverized Coal Based on X-ray Pair Distribution Function

Xiuchao Yang, Zining Zhou, Fang Wu, Jiaxun Liu*

School of Mechanical Engineering, Shanghai Jiao Tong University, Shanghai, China

Abstract

Resolving the atomic structure information of the aromatic layers in coal plays a crucial role in understanding the generation mechanisms of NOx during coal combustion and further reducing the formation of NOx from the source. This study reveals the distribution of X-ray diffraction bands of superfine pulverized coal using a high-resolution synchrotron radiation X-ray Diffraction (HRXRD) facility, discussing the distribution of atomic distances and atomic density in aromatic layers through pair distribution function (PDF) methods. Furthermore, the influences of mechanochemistry on the evolution of atomic morphology are focused on. The results show that the PDF of coal gradually stabilizes when r > 8 Å, showing the short-range order of graphite-like structure. Additionally, due to the limitations of scanning angle and X-ray energy, atomic distances in aromatic layers for coal are significantly greater than that of pure graphene. Enhanced mechanochemical effects make the peaks 1, 2, and 3 of coal PDF more similar to graphene's by condensing alkyl side chains into smaller, regular aromatic layers when the particle size decreases. With the enhancement of mechanochemical effects, coals with different metamorphic degrees exhibit different aromatic evolution patterns. The aromaticity of NMG coal first decreases and then increases, while the aromaticity of YQ coal shows the opposite trend. The results can provide deeper insights into the atomic structure of coal macromolecular, which can facilitate the advancement of novel ultra-low NOx combustion methods and support the construction of precise coal macromolecular models.

Keywords

Superfine Pulverized Coal, Mechanochemistry, HRXRD, PDF

1. Introduction

Coal, as a fossil fuel, has been a cornerstone of human development for centuries. Its abundant reserves and pivotal role in the global energy mix underscore its significance. Despite the rise of renewable energy sources, coal continues to dominate energy consumption patterns worldwide due to its vast availability and established extraction and utilization infrastructure [1-3]. This prominence in the global energy landscape highlights the necessity of understanding and optimizing its use to meet the growing energy demands while mitigating environmental impacts.

Among the various methods of coal utilization, coal combustion still occupies a dominant position. However, combustion has significant environmental implications, especially concerning air quality [4, 5]. Among the pollutants emitted during coal combustion, nitrogen oxides (NOx) are of particular concern due to their detrimental effects on human health

*Corresponding author: liujx@sjtu.edu.cn (Jiaxun Liu)

Received: 25 March 2024; **Accepted:** 29 April 2024; **Published:** 13 June 2024

and their contribution to the formation of ground-level ozone and acid rain [5]. The challenge of reducing NOx emissions while maintaining or improving the efficiency of coal combustion has thus become a critical area of research [6]. However, the formation of NOx during coal combustion is intricately linked to the aromatic layer configuration of coal [7, 8]. Therefore, resolving the atomic structure information of the aromatic layers in coal plays a crucial role in understanding the transformation mechanisms of NOx during the combustion process and further reducing the formation of NOx from the source [9].

The carbon in coal mainly includes abundant amorphous side chains and graphite-like structures, accompanied by different heteroatom polycyclic aromatic hydrocarbons containing various defects such as dislocations and heteroatom substitution [10]. Meanwhile, due to the aggregation and stacking effect of aromatic layers, the graphite-like structure exhibits some hexagonal graphite crystal characteristics in spectroscopic tests, which makes it challenging to characterize the structural information of carbon atoms and aromatic layers in coal [11-13]. X-ray diffraction (XRD), a non-destructive detection method, is widely used to study the crystal structure, phase transformation, and composition of materials [14, 15]. Ismagilov et al. analyzed the amorphous carbon and mineral composition of coal using X-ray diffraction, determining that calcium and silicon exist in amorphous and ionic states in organic compounds of humic acid and fulvic acid [16]. The results promoted the process of coal being used for catalytic hydrogenation cracking of heavy oil.

To investigate the atomic structure information in coal, the atomic pair distribution function (PDF) is used to differentiate the short-range ordered structure, bonding forms, and defects in coal [17]. Simultaneously, PDF can acquire the radial atomic distribution state of a substance by analyzing large-angle and high-resolution XRD data. The high-resolution XRD data is usually obtained through synchrotron radiation facilities, more precisely reflecting the distribution density of radial atoms [17, 18]. Furthermore, by comparing the peak value of PDF with the general bond length, the fine local atomic structure arrangement, including the vacancy and heterotopic defects of the substance in or between the aromatic layer, can be revealed [19, 20]. Marcano et al. used the PDF method to simulate the constructed coal large aromatic layer model [21]. The simulation results were consistent with the experimental results, verifying the reliability of the model. Additionally, peak deviation indicates the presence of heterocyclic aromatic hydrocarbons. Grigoriew et al. studied coal with different degrees of metamorphism using RDF (a deformation of PDF) and found that coal transformed from a structure between diamond and graphite to a diamond structure [22]. Besides, a diamond carbon film structure was also discovered in studying local fine structures. Generally, these conclusions promote the microscopic understanding of atomic structure information in coal.

Superfine pulverized coal is a pulverized coal with a particle size of less than 20μm. Compared with traditional pulverized coal, superfine pulverized coal has advantages such as good combustion stability, high efficiency, and low NOx emissions [23]. Combined with existing low nitrogen combustion technologies such as staged combustion and flue gas recirculation combustion, superfine pulverized coal has enormous industrial application value [24]. However, current research on superfine pulverized coal mainly focuses on qualitative inference at the macro level, lacking understanding at the micro atomic level, which hinders the development of new low NOx combustion technologies [25].

Here, the distribution of X-ray diffraction bands of superfine pulverized coal on a high-resolution synchrotron radiation X-ray Diffraction (HRXRD) facility. The distribution of atomic distances and the atomic density in aromatic layers are discussed combined with PDF methods during superfine grinding. Furthermore, the influences of mechanochemistry on the evolution of atomic morphology are focused on. The results can deepen the understanding of the atomic level of coal physicochemical structure, which can promote the development of new ultra-low NOx combustion technologies and also contribute to the construction of accurate coal macromolecular models.

2. Materials and Methods

2.1. Materials

A typical anthracite coal from Yangquan Coal Industry (Group) Co., Ltd. (YQ) and a bituminous coal from Inner Mongolia Mengxing Coal Mining Co., Ltd. (NMG) were chosen for the experiments to compare the difference of coalification degree. By changing the frequency and duration time, each coal sample was ground in a ball mill to four different equivalent average particle sizes (5.4μm, 17.3μm, 24.0μm, 38.9μm for YQ coal, whereas 12.6μm, 15.0μm, 25.9μm, 52.8μm for NMG coal). The proximate and ultimate analysis of coal samples are shown in Table 1. The ultimate analysis is measured with Vario ELIII (Elemental Analyzer, Germany), while the proximate analysis is performed in accordance with the International Standard ASTM D5373-1 [26].

Table 1. *Proximate and Ultimate Analysis.*

Samples	Proximate analysis (ad) (wt %)		Ultimate analysis (ad) (wt %)	
YQ	M	1.06	C	79.07
	V	7.98	H	3.47
	A	12.43	O	1.01
	FC	78.53	N	1.14

Samples	Proximate analysis (ad) (wt %)		Ultimate analysis (ad) (wt %)	
			S	1.82
	M	14.72	C	54.82
	V	35.69	H	4.39
NMG	A	10.64	O	14.58
	FC	38.95	N	0.63
			S	0.22

*ad represent air dry basis, while O content is calculated by difference.

2.2. High-resolution Synchrotron Radiation X-ray Diffraction (HRXRD) Facility

HRXRD experiments were performed on the synchrotron radiation XRD instrument (beamline BL14B1) at the Shanghai Synchrotron Radiation Facility (SSRF). This facility uses Si (111) and magnetic constraints to filter out monochromatic, collimated X-ray beams, which makes the X-ray beam highly collimated, high-resolution, and high-throughput. The output energy range is 4~22keV, and the energy resolution is 2×10^{-4}@10keV. The wavelength of X-rays is 1.24 Å, and the spot size is 0.5 ×0.5 mm. The diffraction angle range is 6 - 55 degrees (2θ). The step size is 0.01 degrees, and the scanning speed is 0.02 °/s.

2.3. Pair Distribution Function (PDF) Theory

PDF is a concept in statistical physics that represents the radial distribution state of atoms around an atom, as shown in Equation (1) [17].

$$G(r) = 4\pi r(\rho(r) - \rho_0) \quad (1)$$

where ρ(r) is the radial atomic number density of the PDF, while ρ_0 represents the average atomic number density in the system.

Furthermore, $G(r)$ consists of intramolecular pair distribution function $g(r)_{intra}$ and intermolecular pair distribution function $g(r)_{inter}$ $g(r)_{intra}$ and $g(r)_{inter}$ is defined as Equation (2) and Equation (3), respectively [21].

$$g(r)_{intra} = (1-\delta_{\alpha\gamma})\left[\delta(r - r_i^{\alpha} + r_i^{\gamma})\right] \quad (2)$$

where r_i^{α} denotes the immediate spatial location of the αth reference atom within the ith coal molecule. The notation enclosed in angle brackets signifies the average over an equilibrium ensemble, while the inclusion of the Kronecker delta function serves to confirm the distinction between atoms (i.e., $\alpha \neq \gamma$) within an identical coal molecule.

$$g(r)_{inter} = \rho^{-2}\left[N(N-1)\delta(r_i^{\alpha})\delta(r_j^{\gamma} - r)\right] \quad (3)$$

where ρ, defined as N/V, quantifies the mean molecular density per unit volume. The formulation presented in Equation (3) delineates the probability density of intermolecular interactions between atoms α and γ in molecules i and j. Additionally, the comprehensive pair distribution function, G(r), is constituted by the sum of intramolecular and intermolecular components, as presented in Equation (4).

$$G(r)=g(r)_{intra} + g(r)_{inter} \quad (4)$$

Furthermore, by performing background subtraction and normalization on HRXRD data, the diffraction spectrum band of the atom on the X-rays in the coal macromolecular structure can be obtained (Figure 1). Then, PDF function, $G(r)$, varying with the interatomic distance r, is derived using PDFget3 fitting. In addition, to compare the PDF function of coal with the standard PDF functions of graphite and graphene, the PDF functions of graphite and graphene are also provided based on PDF card 41-1487 and the data of Ref. [27].

3. Results

3.1. Distribution of X-ray Diffraction Bands

Figure 1 illustrates the variation of the X-ray diffraction spectrum with the diffraction angle θ. For all coals, the 002 and 100 X-ray diffraction bands are observed. Since the wavelength in the HRXRD experiment is 1.24 Å, the position of the corresponding 002 and 100 diffraction bands is advanced compared with other XRD studies [28].

It is widely accepted that 002 diffraction band is associated with alkyl and aryl carbons in the macromolecular structure of coal. In contrast, the stacking distance of aromatic layers primarily contributes to 100 diffraction band. Compared with YQ coal, NMG coal has a lower coalification degree, which corresponds to massive amorphous carbon atoms existing in the macromolecular of NMG coal. Therefore, the 002 diffraction band of NMG coal is broader than that of HN coal. It is noteworthy that there are no significant differences between the 100 diffraction bands of the two coals, suggesting that the stacking distances of aromatic layers in both coals are similar. In addition, the similar number and position of sharp peaks on the diffraction spectrum of the two coals indicate that the mineral compositions in NMG and HN coal are proximate, which is consistent with the ash content in Table 1. On the other hand, the change of the HRXRD diffraction spectrum with particle size of coals is not apparent. Therefore, to obtain the atomic structure information of different coals, the analyses of PDF function for different coals are conducted in the following sections.

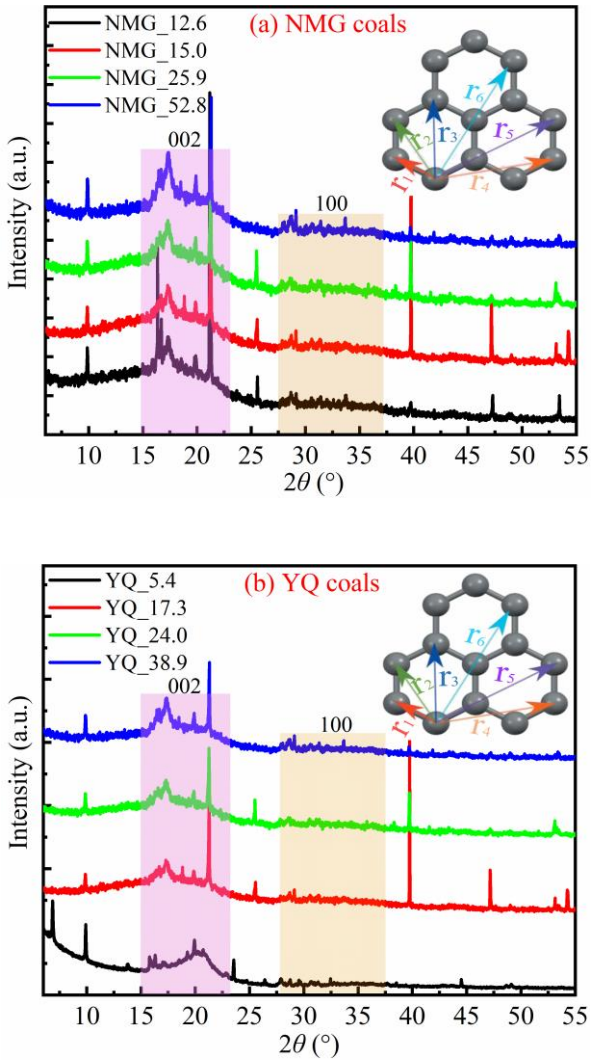

Figure 1. *X-ray diffraction spectrum of two coals.*

3.2. Distribution of Atomic Distances in Aromatic Layers

Figure 1 illustrates the PDF function of all samples. For all coals, when r is greater than 8 Å, the oscillation of the PDF function gradually stabilizes, which implies that the coal molecular structure has a short-range order. Compared with the PDF function of graphene and graphite, the PDF function of pulverized coal displays five significant peaks (peaks 1, 2, 3, 4, and 6) at the corresponding positions, indicating that the aromatic layers of the pulverized coal have a graphite-like structure [29]. Interestingly, the peak intensity after peak 6 is relatively weaker, indicating that the aromatic layers of coal are primarily composed of heptagonal rings combined with Figure 3 [18]. On the other hand, the edge carbon atoms of a single aromatic layer may have unsaturated structures, which facilitate the occurrence of aromatic layer cross-linking reactions during coalification and further induce changes in parameters such as distance and angle between the edge carbon atoms and the central carbon atom. As a result, the relationship between edge carbon atoms and central carbon atoms becomes complex, which makes it difficult to detect the distance between them. According to Figure 3, the r_5 belongs to the category of edge carbon atoms of aromatic layers. Therefore, compared with graphite or graphene, there is no peak 5 on the PDF function of pulverized coal. In addition, under high temperatures and pressure during coalification, the attack of reactive free radicals on the edge carbon atoms of aromatic layers causes the C-C bonds in the rings to break, which may induce the loss of edge carbon atoms. Furthermore, the missing carbon atoms may also contribute to the absence of peak 5 on the coal PDF function. However, the detachment of edge carbon atoms from aromatic layers may also form edge or vacancy reaction defects. It has been demonstrated that defects in aromatic layers are centers of chemical reactions due to the higher electronegativity. Thus, from the perspective of chemical reactivity, the absence of edge carbon atoms is advantageous for the industrial application of coal. Besides, as shown in Figure 1, the X-ray diffraction spectrum presents several sharp peaks, which are contributed by the minerals in the pulverized coal. Consequently, the minerals may also have an effect on the absence of peaks 5 in Figure 2.

Furthermore, the central positions corresponding to each peak are recorded, as listed in Table 2. It can be found that the peak position of coal is higher than the corresponding peak position of graphite or graphene. As mentioned above, the absence of some carbon atoms in the aromatic layers of coal increases the average distance between carbon atoms, which can contribute to the higher peak positions of the coal PDF. Besides, the localized twisting and deformation of aromatic layers may also widen the angles between carbon atoms, which could also influence the detection of carbon atom distances [21]. On the other hand, although minerals can alter the morphology of aromatic layers to some extent, further research is needed to understand how they affect the distance between carbon atoms in aromatic layers [21]. More importantly, the scanning angle and X-ray energy are not sufficiently high, which can also lead to fitting errors in the PDF function. Therefore, this study primarily conducts a qualitative analysis of the atomic structure of coal aromatic layers.

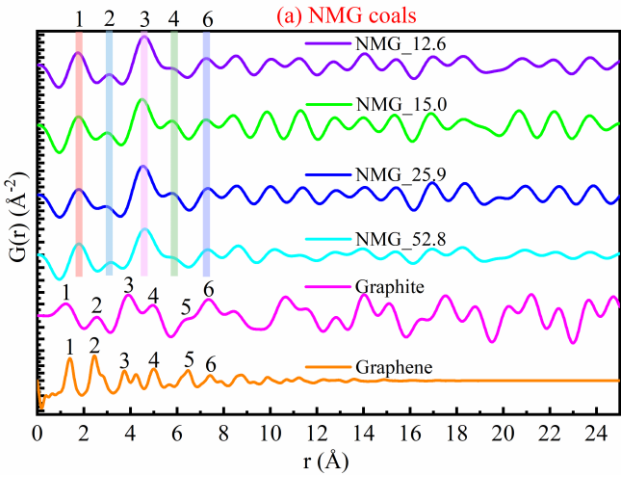

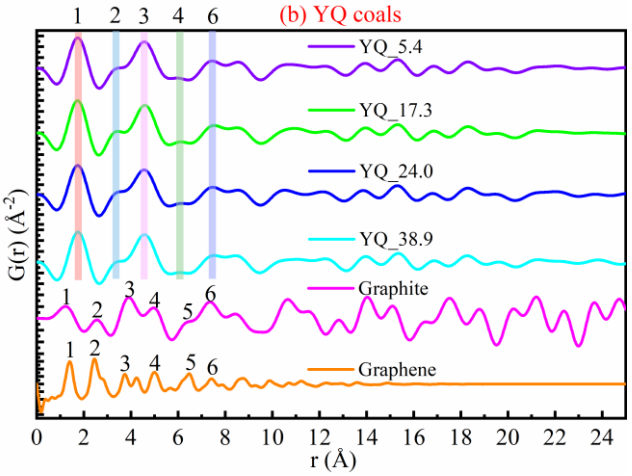

Figure 2. *PDF functions of two coals.*

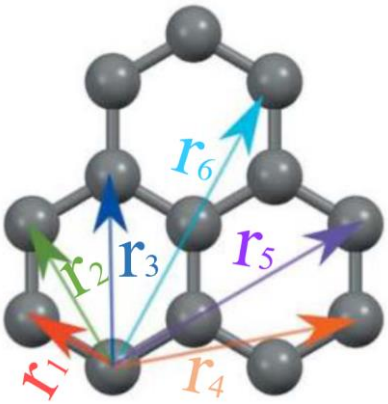

Figure 3. *Atomic distance corresponding to the PDF function peaks.*

Table 2. *Peak positions of PDF function.*

	Peak positions (Å)			
	NMG_12.6	**NMG_15.0**	**NMG_25.9**	**NMG_52.8**
Peak 1	1.75	1.77	1.78	1.79
Peak 2	3.09	3.00	2.94	3.17
Peak 3	4.60	4.50	4.54	4.62
Peak 4	5.69	5.77	5.78	5.76
Peak 6	7.26	7.25	7.32	7.32
	YQ_5.4	YQ_17.3	YQ_24.0	YQ_38.9
Peak 1	1.75	1.74	1.75	1.78
Peak 2	3.45	3.44	3.44	3.46
Peak 3	4.57	4.57	4.58	4.52
Peak 4	5.96	6.16	6.08	5.98
Peak 6	7.45	7.48	7.53	7.57

Based on Figure 2, for all coals, it can be observed that peaks 1, 2, and 3 are the most prominent. Moreover, the first three peaks in the PDF functions correspond to separation distances between pairs of atoms within the same polyaromatic structure [21]. Therefore, the following section focuses primarily on the comparative analysis of peaks 1, 2, and 3. During superfine grinding, the decrease in particle size is accompanied by the increased grinding energy, which induces the mechanochemical effects between the atomic structure [30]. Furthermore, the mechanochemical effects result in the cleavage of some weakly stable alkyl side chains, further condensing into smaller aromatic layers under high temperature and pressure [30]. As a result, the proportion of small aromatic layers in small particles increases as the particle size decreases. Simultaneously, the morphology of those new small aromatic layers is also more regular due to less interference from alkyl side chains. Therefore, the position of peak 1, 2, and 3 is generally closer to that of pure graphene with the decrease in particle size except for peak 3 of YQ coal. Moreover, the corresponding peak positions also exhibit a decreasing trend during the particle size reduction. However, the position of peak 3 for YQ coal has an upward trend with the decrease in particle size, which may be due to the fracture of the large-span aromatic layer in YQ coal with higher coalification degree during superfine grinding, resulting in more aromatic clusters squeezing the aromatic rings. It needs to be pointed out that peaks observed at r > 5 Å are influenced by stacking and adjacent clusters (intramolecular contribution), complicating the analysis of the PDF function. Consequently, the position of peaks 4 and 6 lack an obvious pattern of evolution.

From the perspective of the coalification degree, the position of peak 1 can be considered a qualitative criterion. Theoretically, the distance of aryl C-C bonds is 1.39 Å, while the distance of alky C-C bonds is 1.54 Å [21]. Table 1 indicates that the position of peak 1 in YQ coal is significantly lower than that of peak 1 in NMG coal, suggesting that YQ coal has a higher degree of coalification. This is consistent with the results of the proximate analysis presented in Table 1.

3.3. Evolution of Aromatic Carbon Atom Content

The peak amplitude in PDF has a strong correlation with coal rank [21]. More specifically, the peak amplitude increases with the increasing coal rank. As mentioned above, according to the peak distribution in Figure 2, for all coals, it can be observed that peaks 1, 2, and 3 are the most prominent peaks. Moreover, the first three peaks in the PDF functions correspond to separation distances between pairs of atoms within the same polyaromatic structure. However, peaks 4 and 6 are influenced by stacking and adjacent clusters (intramolecular contribution), complicating the types of aromatic carbon atoms. On the other hand, after statistical analysis, the amplitude of peak 2 has negative values, which

could introduce significant errors in the discussion of aromatic carbon atoms. Therefore, the following section primarily analyzes the morphology of aromatic carbon atoms through the evolution of peaks 1 and 3.

Figure 4 presents the evolution of peak amplitude with particle size. Different coal has varying evolutionary trends. NMG coal, with a lower coalification degree, contains a large amount of amorphous carbon. As the particle size initially decreases, the alkyl side chains in NMG coal first fall off to form reactive fragments, accompanied by the breaking of carbon atoms at the edges of the aromatic layers. Consequently, the number of aromatic carbon atoms decreases. With further reduction in particle size, those detached reactive fragments recondense into aromatic rings under the action of mechanochemistry, increasing the content of aromatic carbon. Therefore, for NMG coals, the amplitude of peaks 1 and 3 decreases first and then increases with the reduction of particle size. However, the Physicochemical structure of YQ coal with a higher coalification degree is relatively dense, which reduces the active space of amorphous carbon that falls off during superfine grinding. Consequently, as the initial particle size decreases, the detached small molecular fragments can quickly condense into aromatic rings, which induces an increase in amplitude of peaks 1 and 3. As the particle size is further reduced, longitudinal shear forces gradually become dominant compared with transverse shear forces. The longitudinal shear forces can shear the edge carbon atoms of the aromatic layers, thereby inducing a reduction in aromatic carbon. Therefore, generally, the amplitude of peaks 1 and 3 in YQ coal shows a trend of first increasing and then decreasing with the reduction of particle size. Furthermore, when the particle size is between 15.0-25.9μm, the amplitude of peaks 1 and 3 for NMG coal exhibits a minimum value. In comparison, the amplitude of corresponding peaks in YQ coal presents a maximum value in the particle size range of 17.3-24.0μm. Additionally, due to the higher coalification degree, YQ coal has a greater peak amplitude than that of NMG coal.

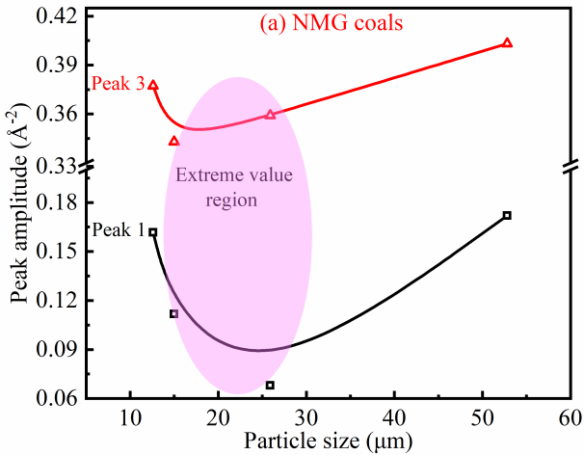

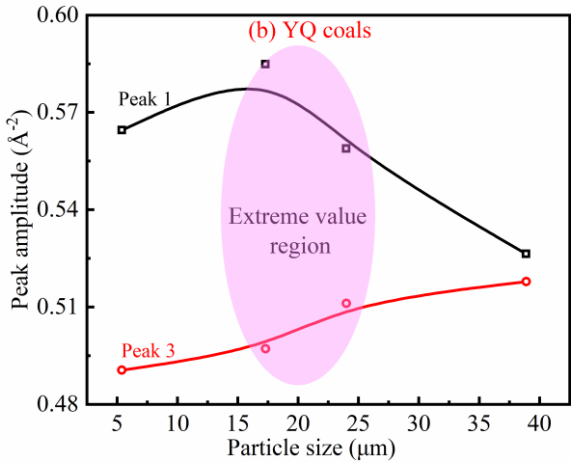

Figure 4. *Peak amplitude of PDF functions.*

4. Discussion

The PDF function can resolve the carbon atomic structure information of the aromatic layer in coal, which can contribute to the industrial application and establishment of macromolecular models. However, coal is a highly complex polymer with a complex physical and chemical structure. In addition to containing massive carbon-containing organic matter, coal also includes abundant minerals. Figure 5 shows the three key factors affecting coal PDF function. During coalification, high temperatures and pressure cause mutual compression between aromatic layers, which induces the deformation of aromatic layers, such as distortion, cleavage, and rotation. The deformation significantly affects the statistical distance of carbon atoms in the aromatic layer through the PDF. In addition, during coalification, some active alkyl fragments may attack the aromatic layer, resulting in the loss of some carbon atoms. Furthermore, abundant structure defects like edge defects, surface vacancy defects, including single and double vacancy defects, Stone-Wales defects, and heteroatom substitution defects, are generated due to the loss of carbon atoms, which further leads to the leads to a change in the delocalized state of π electrons on aromatic rings. Consequently, the atom distance will also be affected. Besides, the minerals in coal may also affect the distribution of atomic distance in the aromatic layer by altering the form of aromatic rings. It is worth noting that this study primarily conducts a qualitative analysis of the atomic structure of coal aromatic layers.

High-Resolution Transmission Electron Microscope (HRTEM) can visually detect the disordered morphology of aromatic layers in coal [31]. Molecular dynamics simulation can couple the effects of minerals in coal [19]. Therefore, the combined application of HRTEM, Molecular dynamics simulation, and HRXRD may provide a more comprehensive analysis of atomic structure information in coal, which is worth trying in future research.

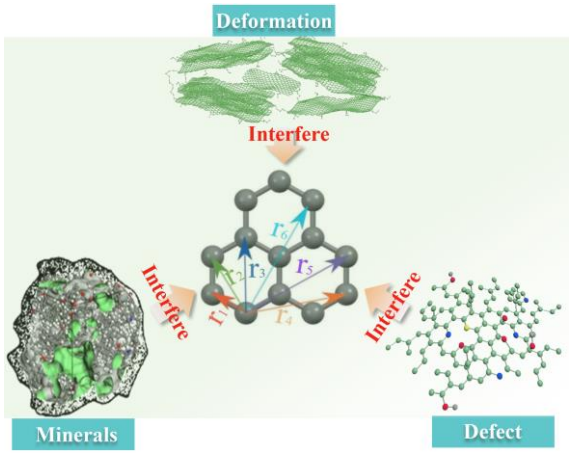

Figure 5. *Key influencing factors of carbon atomic distance in coal.*

5. Conclusions

The PDF of coal gradually stabilizes when r > 8 Å, showing the short-range order of the coal molecular structure. Furthermore, the PDF of coal displays five significant peaks corresponding to the peak position of PDF for graphene and graphite, indicating that the aromatic layers of coal have a graphite-like structure. During superfine grinding, mechanochemical effects condense detached alkyl side chains into smaller and more regular aromatic layers, making the positions of peaks 1, 2, and 3 for coal become closer to those of pure graphene as particle size decreases. Under similar mechanochemical effects, coals with different coalification degrees exhibit varying trends in the aromaticity evolution. When the particle size belongs to 15.0 - 25.9μm, the amplitudes of peaks 1 and 3 in NMG coal reach the lowest, suggesting minimal aromaticity in this particle size range. However, the peak amplitudes of YQ coal are highest at 17.3 - 24.0μm, indicating the larger aromaticity in the size range.

Due to the limitations of scanning angle and X-ray energy, this study primarily conducts a qualitative analysis of the atomic structure. The combined application of HRTEM, molecular dynamics simulation, and HRXRD may provide a more comprehensive understanding of atomic structure information in coal, which is worth trying in future research.

Abbreviations

NOx	Nitrogen Oxides
HRXRD	High-Resolution Synchrotron Radiation X-ray Diffraction
PDF	Pair Distribution Function
HRTEM	High Resolution Transmission Electron Microscope

Supplementary Material

This research has no supplementary materials.

Acknowledgments

We acknowledge the support from the National Natural Science Foundation of China (Grant Nos. 52076133). The authors are grateful to the Shanghai Synchrotron Radiation Facility BL14B1 beamline station for giving the opportunity for the HRXRD experiments.

Author Contributions

Xiuchao Yang: Writing - Original draft preparation, Methodology, Investigation

Zining Zhou: Investigation, Methodology

Fang Wu: Investigation, Methodology

Jiaxun Liu: Writing - Review & Editing, Conceptualization, Supervision, Funding acquisition

Funding

This work is supported by Coal Combustion Ultra-low NOx Formation Mechanism based on Directional Regulation of Macromolecular Aggregation State of Funder (Grant No. 52076133).

Data Availability Statement

The data supporting the outcome of this research work has been reported in this manuscript.

Conflicts of Interest

The authors declare no conflicts of interest.

References

[1] Gao X, Chen H, Wei L, Pan P, Zhang K, Wu L. Performance assessment of a hydrothermal treatment-based sewage sludge-to-electricity system integrated with a coal-fired power plant. Energy Conversion and Management. 2024, 300, 117957. https://doi.org/10.1016/j.enconman.2023.117957

[2] Ogugua PC, Su H, Wang E. Synergistic blending of biomass, sewage sludge, and coal for enhanced bioenergy production: Exploring residue combinations and optimizing thermal conversion parameters. Journal of Environmental Management. 2024, 352, 120035. https://doi.org/10.1016/j.jenvman.2024.120035

[3] Zhou F, Yu J, Wu C, Fu J, Liu J, Duan X. The application prospect and challenge of the alternative methanol fuel in the internal combustion engine. Science of the Total Environment. 2024, 913, 169708. https://doi.org/10.1016/j.scitotenv.2023.169708

[4] Niu S, Han K, Lu C. Release of sulfur dioxide and nitric oxide and characteristic of coal combustion under the effect of calcium based organic compounds. Chemical Engineering Journal. 2011, 168(1), 255-61. https://doi.org/10.1016/j.cej.2010.10.082

[5] Glarborg P, Miller JA, Ruscic B, Klippenstein SJ. Modeling nitrogen chemistry in combustion. Progress in Energy and Combustion Science. 2018, 67, 31-68. https://doi.org/10.1016/j.pecs.2018.01.002

[6] Phiri Z, Everson RC, Neomagus HWJP, Wood BJ. Transformation of nitrogen functional forms and the accompanying chemical-structural properties emanating from pyrolysis of bituminous coals. Applied Energy. 2018, 216, 414-27. https://doi.org/10.1016/j.apenergy.2018.02.107

[7] Yu J, Lucas JA, Wall TF. Formation of the structure of chars during devolatilization of pulverized coal and its thermoproperties: A review. Progress in Energy and Combustion Science. 2007, 33(2), 135-70. https://doi.org/10.1016/j.pecs.2006.07.003

[8] Zhang L, Hu S, Xu K, Jiang L, Wang Y, Su S, et al. Study on the structural evolution of semi-chars and their solvent extracted materials during pyrolysis process of a Chinese low-rank coal. Fuel. 2018, 214, 363-8. https://doi.org/10.1016/j.fuel.2017.11.043

[9] Molina A, Murphy JJ, Winter F, Haynes BS, Blevins LG, Shaddix CR. Pathways for conversion of char nitrogen to nitric oxide during pulverized coal combustion. Combustion & Flame. 2009, 156(3), 574-87. https://doi.org/10.1016/j.combustflame.2008.11.012

[10] Feng B, Bhatia SK, Barry JC. Structural ordering of coal char during heat treatment and its impact on reactivity. Carbon. 2002, 40(4), 481-96. https://doi.org/10.1016/S0008-6223(01)00137-3

[11] Liang D, Singer S. Pore-resolving simulations to study the impacts of char morphology on zone II combustion and effectiveness factor models. Combustion and Flame. 2021, 229, 111405. https://doi.org/10.1016/j.combustflame.2021.111405

[12] Badaczewski F, Loeh MO, Pfaff T, Dobrotka S, Wallacher D, Clemens D, et al. Peering into the structural evolution of glass-like carbons derived from phenolic resin by combining small-angle neutron scattering with an advanced evaluation method for wide-angle X-ray scattering. Carbon. 2019, 141, 169-81. https://doi.org/10.1016/j.carbon.2018.09.025

[13] Zickler GA, Smarsly B, Gierlinger N, Peterlik H, Paris O. A reconsideration of the relationship between the crystallite size La of carbons determined by X-ray diffraction and Raman spectroscopy. Carbon. 2006, 44(15), 3239-46. https://doi.org/10.1016/j.carbon.2006.06.029

[14] Chatterjee A, Maiti P, Siddiqi H, Mishra A, Durga Prasad G, Meikap BC. Interpreting crystallographic and microcrystalline structural effect for demineralization of low-grade thermal coal in multi-stage chemical leaching: A cleaner combustion approach. Powder Technology. 2024, 435. https://doi.org/10.1016/j.powtec.2024.119435

[15] Xu X, Yuan S, Li J, Guo S. Microscopic mechanism of carbon oxides formation during long-flame coal oxidation at molecular scale. Fuel. 2024, 362. https://doi.org/10.1016/j.fuel.2023.130824

[16] Ismagilov ZR, Shigabutdinov AK, Presnyakov VV, Idrisov MR, Khramov AA, Urazaykin AS, et al. Developing Additives Based on Russian Coal for the Thermal Hydrocracking of Heavy Tar 4. X-ray Diffraction Study of Coal Composition. Coke and Chemistry. 2023, 66(10), 485-9. https://doi.org/10.3103/S1068364X23701144

[17] Terban MW, Billinge SJL. Structural Analysis of Molecular Materials Using the Pair Distribution Function. Chemical Reviews. 2022, 122(1), 1208-72. https://doi.org/10.1021/acs.chemrev.1c00237

[18] Wertz DL, Bissell M. One-dimensional description of the average polycyclic aromatic unit in Pocahontas No. 3 coal: an X-ray scattering study. Fuel. 1995, 74(10), 1431-5. https://doi.org/10.1016/0016-2361(95)00107-G

[19] Zhang Z. Structure and dynamics in brown coal matrix during moisture removal process by molecular dynamics simulation. Molecular Physics. 2011, 109(3), 447-55. https://doi.org/10.1080/00268976.2010.528055

[20] Cavallari C, Rols S, Fischer HE, Brunelli M, Gaboardi M, Magnani G, et al. Neutron scattering study of nickel decorated thermally exfoliated graphite oxide. International Journal of Hydrogen Energy. 2019, 44(59), 30999-1007. https://doi.org/10.1016/j.ijhydene.2019.09.226

[21] Castro-Marcano F, Winans RE, Chupas P, Chapman K, Calo JM, Watson JK, et al. Fine structure evaluation of the pair distribution function with molecular models of the Argonne Premium coals. Energy and Fuels. 2012, 26, 4336-45. https://doi.org/10.1021/ef300364e

[22] Grigoriew H. Interpretation of the pair function for laminar amorphous materials in the case of coals. I. Model considerations. Journal of Applied Crystallography 1988, 21(2), 97-101. https://doi.org/10.1107/S0021889887009890

[23] Liu J, Jiang X, Shen J, Zhang H. NO emissions from oxidizer-staged combustion of superfine pulverized coal in the O_2/CO_2 atmosphere. Energy and Fuels. 2014, 28(8), 5497-504. https://doi.org/10.1021/ef5009924

[24] Liu J, Jiang X, Shen J, Zhang H. Pyrolysis of superfine pulverized coal. Part 3. Mechanisms of nitrogen-containing species formation. Energy Conversion and Management. 2015, 94, 130-8. https://doi.org/10.1016/j.enconman.2014.12.096

[25] Shen J, Liu J, Xing Y, Zhang H, Luo L, Jiang X. Application of TG-FTIR analysis to superfine pulverized coal. Journal of Analytical and Applied Pyrolysis. 2018, 133, 154-61. https://doi.org/10.1016/j.jaap.2018.04.007

[26] ASTMD5373−16, Standard Test Methods for Determination of Carbon, Hydrogen and Nitrogen in Analysis Samples of Coal and Carbon in Analysis Samples of Coal and Coke; ASTM International: West Conshohocken, PA, 2016.

[27] Pol VG, Calderon-Moreno JM, Chupas PJ, Winans RE, Thiyagarajan P. Synthesis of monodispersed prolate spheroid shaped paramagnetic carbon. Carbon. 2009, 47(4), 1050-5. https://doi.org/10.1016/j.carbon.2008.12.028

[28] Wang C, Zeng F, Li C, Xu Q, Chen P. Insight into the molecular structural evolution of a series of medium-rank coals from China by XRD, Raman and FTIR. Journal of Molecular Structure. 2024, 1303. https://doi.org/10.1016/j.molstruc.2024.137616

[29] Saikia BK. Inference on carbon atom arrangement in the turbostatic graphene layers in Tikak coal (India) by X-ray pair distribution function analysis. International Journal of Oil, Gas and Coal Technology. 2010, 3(4), 362-73. https://doi.org/10.1504/IJOGCT.2010.037465

[30] Luo L, Yao W, Liu J, Zhang H, Ma J, Jiang X. The effect of the grinding process on pore structures, functional groups and release characteristic of flash pyrolysis of superfine pulverized coal. Fuel. 2019, 235, 1337-46. https://doi.org/10.1016/j.fuel.2018.08.081

[31] Zhong Q, Mao Q, Zhang L, Xiang J, Xiao J, Mathews JP. Structural features of Qingdao petroleum coke from HRTEM lattice fringes: Distributions of length, orientation, stacking, curvature, and a large-scale image-guided 3D atomistic representation. Carbon. 2018, 129, 790-802. https://doi.org/10.1016/j.carbon.2017.12.106

Biography

Xiuchao Yang is a current Ph.D. student at the School of Mechanical and Power Engineering, Shanghai Jiao Tong University. He graduated with a master's degree from Harbin Institute of Technology in 2018. He has a distinguished record of publishing in top journals within the combustion field, including Fuel, Energy, and Fuel Processing Technology. His research primarily focuses on novel coal combustion technologies, ultra-low NOx emission techniques, and the microstructure of carbon-based materials. His work contributes significantly to advancements in energy efficiency and environmental protection.

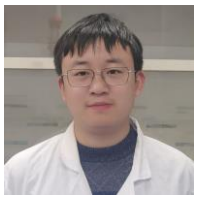

Zining Zhou graduated with a bachelor's degree from Southeast University. He is currently studying at the School of Mechanical and Power Engineering, Shanghai Jiao Tong University, pursuing a master's degree. The current research direction includes Novel technology of coal combustion, Control of combustion pollutants and Dynamic characterization of pore structure.

Fang Wu received bachelor's degree in energy and power engineering from Shanghai Jiao Tong University, currently continues his studying to pursue a doctor's degree at the School of Mechanical Engineering, Shanghai Jiao Tong University. His research direction is mainly related to thermal catalysis of carbon-based materials.

Jiaxun Liu is an Associate Researcher at the School of Mechanical and Power Engineering, Shanghai Jiao Tong University. He acquired his Ph.D. from Harbin Institute of Technology in 2011. In 2019, he was a recipient of the Shanghai Jiao Tong University Morning Star Associate Professor B Class Support Program. Dr. Jiaxun Liu has made significant contributions to the field of environmental and energy sciences, with a total of 84 publications in top international journals such as Environmental Science & Technology, Combustion and Flame, Fuel, Energy, and Energy Conversion and Management. In addition to his research work, he has been an active peer reviewer for multiple journals, earning the "Valuable Contribution and Dedicated Service in The Peer Review of Manuscripts Submitted to ACS Journals" honor from the American Chemical Society in 2011.

Research Field

Xiuchao Yang: Novel technology of coal combustion, Control of combustion pollutants, Research on aggregated molecular dynamics, Carbon material microstructure detection, Quantum chemical simulation of combustion.

Zining Zhou: Novel technology of coal combustion, Control of combustion pollutants, Dynamic characterization of pore structure, Quantum chemical simulation of combustion, Application of advanced materials for carbon reduction.

Fang Wu: Research on seaweed biomass and bioenergy, Biomass thermal catalytic conversion, Molecular dynamics simulation, Control of combustion pollutants, Application of advanced materials for carbon reduction.

Jiaxun Liu: Application of advanced materials for carbon reduction, Research on seaweed biomass and bioenergy, Novel technology of coal combustion, Research on the characteristics of combustion radicals, Pathogenic mechanism of combustion particulate matter.